Conformal coating of particles in microchannels by magnetic forcing

Scott S. H. Tsai, Jason S. Wexler, Jiandi Wan, and Howard A. Stone

Citation: Appl. Phys. Lett. **99**, 153509 (2011); doi: 10.1063/1.3652772
View online: http://dx.doi.org/10.1063/1.3652772
View Table of Contents: http://apl.aip.org/resource/1/APPLAB/v99/i15
Published by the American Institute of Physics.

Conformal coating of particles in microchannels by magnetic forcing

Scott S. H. Tsai,[1] Jason S. Wexler,[2] Jiandi Wan,[2] and Howard A. Stone[2,a)]
[1]*School of Engineering and Applied Sciences, Harvard University, Cambridge, Massachusetts 02138, USA*
[2]*Department of Mechanical and Aerospace Engineering, Princeton University, Princeton, New Jersey 08544, USA*

(Received 18 August 2011; accepted 22 September 2011; published online 14 October 2011)

We present a co-flow microfluidic method to coat paramagnetic beads with a thin layer of fluid as the beads are pulled across a liquid-liquid interface by an external magnetic field. We show that the coating thickness can be controlled by the magnitude of the flow speed. Also, the number of beads aggregated within a single coating can be adjusted by varying the strength of the magnetic field or the liquid-liquid interfacial tension. © *2011 American Institute of Physics*. [doi:10.1063/1.3652772]

Coating of microparticles is useful in many technologies. For example, coating of cells has found application in drug delivery where the coating layer acts as a drug-carrying vehicle and/or a protective barrier against the host's immune system.[1,2] Indeed, the need for high-throughput, tunable, and ultra-thin coatings is a roadblock to improved drug delivery and cell therapy,[3] making the development of an approach for coating micron-scale objects very desirable.

Discrete coatings of objects have been demonstrated in the past using selective withdrawal[4] and centrifugal[1] and magnetic[2] conformal coating. Whether and how similar approaches can be integrated to be useful in microfluidic settings has not been considered. Given all of the benefits of miniaturization[5] and the development of microfluidic capabilities such as sorting[6] and encapsulation,[7] a microfluidic technique for particle coating would enhance the usefulness of lab-on-a-chip devices.

Here we introduce a microfluidic technique that can controllably coat micron-scale beads with $O(1\ \mu m)$ thick liquid layers and vary the number of beads trapped inside the coating layer. Our proposed method takes advantage of features similar to classical fluid mechanics problems such as the approach of a solid sphere toward[8,9] and across[10,11] a liquid-liquid interface by gravitational forcing, where a discrete volume of liquid can be entrained on the sphere. This approach is distinguished from typical descriptions of coating flows where a continuous film is forced over a solid surface via a relative motion.[12,13] Since gravitational effects are weak in microfluidics, we apply magnetic forces to move the beads in our experiments, drawing on ideas from magnetic separations.[6,14] In particular, we accomplish the coating by forcing the particles across a liquid-liquid interface.

The microfluidic device is made using standard soft-lithography methods[15] with polydimethylsiloxane (PDMS, Sylgard 184 silicone elastomer kit, Dow Corning) bonded to a glass microscope slide. All channels have a constant height of 50 μm, and the coating region has a width of 380 μm. Fig. 1(a) shows the flow-focusing geometry[16] of the aqueous phase that centers the beads laterally in the channel so that all of the beads cross the interface at approximately the same location. The non-aqueous (oil) solution enters through a second inlet and forms a co-flow with the aqueous phase.

The non-aqueous solution consists of dodecane with 10 wt. % sorbitan monooleate surfactant (Span 80), while the aqueous solution is a mixture of deionized water with varying concentrations of sodium dodecyl sulfate (SDS). This combination produces an ultra-low interfacial tension,[17] which is below the minimum value of 1 mN/m measurable with equipment we have available. The aqueous and non-aqueous solutions have viscosities of 1 and 2.7 mPa s, respectively. The paramagnetic beads have a radius of $R = 2.5\ \mu$m and are composed of a polystyrene matrix embedded with iron oxide nanoparticles (Sigma). The hydrophilic beads are suspended at a volume fraction of 0.06% in the aqueous solution, which flows through one inlet, while the same fluid without the suspension flows through a separate inlet [labeled "buffer" in Fig. 1(a)]. Constant flow-rate syringe pumps (Harvard Apparatus) provide the same flow-rate to each inlet. The experiments are imaged using bright-field microscopy (Leica) with a $63\times$ oil immersion objective (NA = 1.4) and a high-speed camera (Vision Research).

A stack of three neodymium iron boron magnets (K. J. Magnetics), each with magnetization 1 MA/m and dimensions $9.5 \times 4.8 \times 1.6$ mm, is used to deflect the beads through the liquid-liquid interface. A slot is cut in the PDMS before bonding to the glass to allow the magnets to be placed at approximately $\delta \approx 1$ mm from the edge of the flow channel [Fig. 1(a)]. As the magnetic beads enter the region of

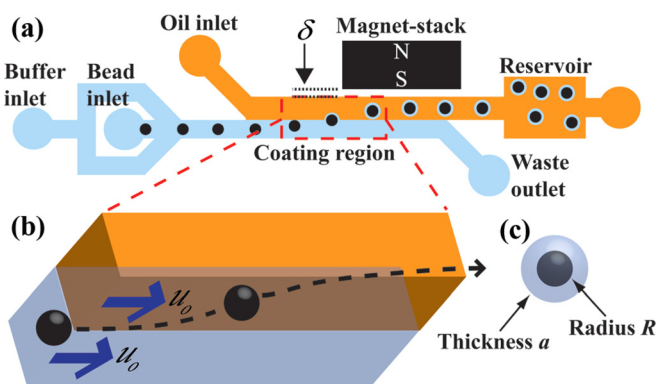

FIG. 1. (Color online) (a) Schematic of the microfluidic device with a co-flow geometry where the aqueous solution flows through the buffer inlet while magnetic beads enter through a separate inlet. Dodecane with 10 wt. % Span 80 flows through the oil inlet. (b) A magnet adjacent to the device deflects the beads from the aqueous phase into the oil phase. (c) The beads end up coated with a thin aqueous layer.

a) Author to whom correspondence should be addressed. Electronic mail: hastone@princeton.edu.

influence of the magnet-stack, they are pulled from the aqueous phase into the non-aqueous phase, penetrating through the liquid-liquid interface [Fig. 1(b)]. The beads retain a thin coating of the original fluid [Fig. 1(c)].

The film thickness is estimated with IMAGEJ software by subtracting the measured bead diameter from the measured diameter of the coating layer and dividing by two. Two film thickness values in perpendicular directions are measured for each bead and we report the average value. We were able to measure film thickness as small as approximately 500 nm, since both the bead diameter and the coating layer diameter are significantly larger than the 200 nm resolution of our objective. We always took measurements at the same focal plane relative to the particle to reduce experimental error.

Beads flowing with the fluids from left to right are deflected by the external magnetic field as shown in Fig. 2(a). The experimental image shows the liquid-liquid interface of co-flowing dodecane (top) and 8 mM SDS in water (bottom) solutions. The beads deform the interface and then penetrate through it. As the beads move away from the interface, the entrained fluid undergoes a sequence of events. First, a thread is formed [Fig. 2(b)] and breaks up into drops by the Rayleigh-capillary instability [Fig. 2(c)]. Second, there is continual deformation [Fig. 2(d)] and breakup [Fig. 2(e)] at the back of the comet-shaped tail. The latter interface deformation resembles a shear-driven process known as tip-streaming that has been reported extensively in the literature.[18] Since the height of the magnet-stack (4.8 mm) is much larger than the height of the channel ($h \approx 50\,\mu$m), there is a vertical gradient of magnetic field, which causes the beads to be pulled to the top of the channel. As a result, the beads lag by a factor κ relative to the average flow speed u_o in both fluid phases, where κ is an order one constant. In the reference frame of the moving fluid, the beads are moving in both parallel $(-\kappa u_o)$ and perpendicular $(u_\perp)$ directions, and drops are emitted from the tail in the diagonal direction as evident in Fig. 2(e). We hypothesize that it may be possible to reduce the speed-lag κ by using a thin magnet that produces a weaker vertical gradient of magnetic field, and proof-of-concept experiments show the beads moving only transverse to the flow (see Fig. S1 in supplementary material[19]).

We observe a decrease in the coating thickness a as we increase the average flow speed u_o and plot the dimensionless coating thickness a/R versus u_o; see Fig. 2(f). As shown in the log-log plot in the inset, our results follow an empirical trend $a/R \propto u_o^{-1/2}$. We expect that by increasing u_o, we increase the beads' total speed $u_p^2 = (\kappa u_o)^2 + u_\perp^2$ relative to the flow [Fig. 2(e)], and we recall for viscous flows that the shear stress τ increases proportionally with u_p. We expect that these stresses cause a reduction in the coating thickness, though we are not aware of any model to date of such a flow. We also measure a coating rate of approximately 100 beads/s, while performance limitations are related to the magnet's size and strength, and the bead concentration above which particle-particle interactions cause the beads to aggregate prior to approaching the interface.

The number of beads inside a single coating can also be controlled. Fig. 3(a) shows the conformal coating process for a magnet-stack displacement of $\delta \approx 2$ mm: two-bead aggregates are formed and pass through the interface. As δ increases in 1 mm increments from 2 to 4 mm [Figs. 3(b)–3(d)], coatings with larger aggregates are observed. The same trends are seen when the interfacial tension between the two phases is lowered by using an aqueous solution of 2 mM SDS in water [Fig. 3(e)].

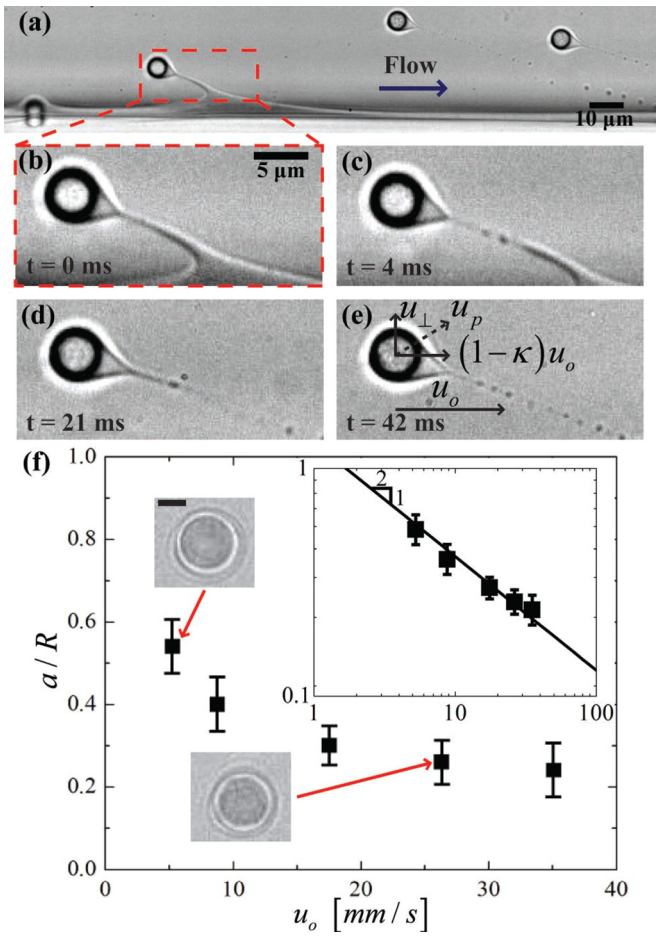

FIG. 2. (Color online) (a) Experimental image of 2.5 μm radius magnetic beads being pulled from a solution of 8 mM SDS in water (bottom) into a solution of dodecane with 10 wt. % Span 80 (top). Magnetic beads are coated conformally as they cross the interface. As the beads move away from the interface, we observe in a time-sequence of images of the same bead, (b) thread formation, (c) the Rayleigh-capillary instability, (d) continual deformation, and (e) tip-streaming. (f) A plot of the dimensionless coating thickness versus the average flow speed for the same solutions and beads shows that coating thickness decreases with increasing speed. The inset shows a log-log plot of the data with a solid line indicating an empirical trend $a/R \propto u_o^{-1/2}$. Error bars represent one standard deviation. Images of beads with dimensionless coating thickness of $a/R = 0.54 \pm 0.07$ and 0.26 ± 0.06 corresponding respectively to flow speeds of $u_o = 5.3$ and 25.3 mm/s are shown. The outer layer is the coating while the bright ring in the middle is an optical artifact. Scale bar 2 μm.

We next address force balances to rationalize the trends in particle number trapped in the coating by examining the ratio of magnetic to surface forces. We consider N particles in a single aggregate where the magnetic forces are $F_m \approx \mu_o \chi L^3 \nabla H^2$ and the surface forces are $F_\gamma \approx \gamma L$, with H the external magnetic field, γ is the interfacial tension between the two phases, $L^3 = NR^3$ is the volume of an aggregate, and μ_o and χ, respectively, are the permeability of free space ($\mu_o \approx 1.257 \times 10^{-6}$ m kg s^{-2} A^{-2}) and the magnetic susceptibility of each bead ($\chi \approx 10^{-3}$). Thus, as a function of particle number, the magnetic and surface forces scale as $F_m \propto N \nabla H^2$ and $F_\gamma \propto \gamma N^{1/3}$. Qualitatively, we observe that

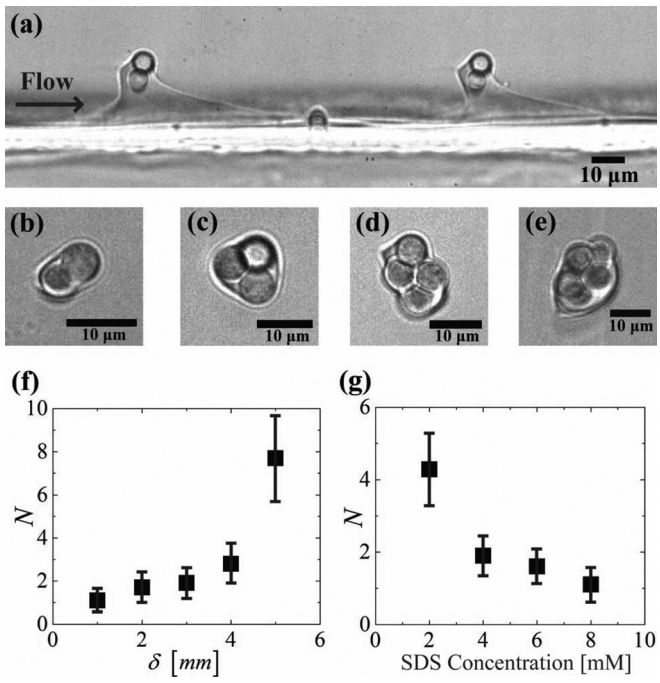

FIG. 3. (a) Image showing the two-phase interface (bottom aqueous, top non-aqueous) and aggregates of beads being pulled through the interface. The magnet-stack is displaced $\delta \approx 2$ mm from the channel. (b)–(e) Representative images when we independently vary δ and the aqueous phase SDS concentration. Scale bars 10 μm. We observe aggregate sizes of (b) 2 beads ($\delta = 2$ mm), (c) 3 beads ($\delta = 3$ mm) and (d) 4 beads ($\delta = 4$ mm) for a constant SDS concentration of 8 mM, and (e) 5 beads (2 mM SDS concentration) for a fixed $\delta \approx 2$ mm. The average number of beads N inside one encapsulation is plotted against (f) the magnet's displacement δ and (g) the SDS concentration in the aqueous phase, which is varied from 2 to 8 mM. N increases monotonically with δ and decreases monotonically with increasing surfactant concentration. Error bars represent one standard deviation.

increasing the displacement δ of the magnet-stack reduces the magnetic force F_m and requires more beads N inside one aggregate to balance the force at the interface F_γ. The same trend applies when the surface tension γ becomes higher with reduced SDS concentration. Both qualitative behaviors are observed in Figs. 3(f) and 3(g), where the number of beads N inside one encapsulation increases monotonically as a function of δ and decreases monotonically as a function of SDS concentration.

The ability to coat particles is an important unit operation in biotechnology and adds to the functional capabilities of lab-on-a-chip devices. We have integrated a conformal coating method into a microfluidic device by driving magnetic beads through a liquid-liquid interface in a two-phase co-flowing channel. Our technique is continuous, tunable in both coating thickness and bead number and achieves a coating thickness of $O(1\ \mu\text{m})$. Our method offers the possibility of coating other discrete objects such as cells by binding the cells to magnetic beads. This approach should also allow for the generation of multiple layers of coatings by either passing the particles across many streams of immiscible fluids or back and forth between aqueous and non-aqueous phases.

We gratefully acknowledge financial support from the NSF (Grant No. NSF-CBET-0961081). We also thank H.C. Shum for advice on the low surface tension solutions, B. Selva for surface tension measurements, and M. Staykova, M. Roche, and J. Nunes for helpful discussions.

[1]M. V. Sefton, M. H. May, S. Lahooti, and J. E. Babensee, J. Controlled Release **65**, 173 (2000).
[2]A. Khademhosseini, M. H. May, and M. V. Sefton, Tissue Eng. **11**, 1797 (2005).
[3]J. T. Wilson and E. L. Chaikof, Adv. Drug Delivery Rev. **60**, 124 (2008).
[4]I. Cohen, H. Li, J. L. Hougland, M. Mrksich, and S. R. Nagel, Science **292**, 265 (2001).
[5]G. M. Whitesides, Nature **442**, 368 (2006).
[6]N. Pamme and C. Wilhelm, Lab Chip **6**, 974 (2006).
[7]J. Wan, A. Bick, M. Sullivan, and H. A. Stone, Adv. Mater. **20**, 3314 (2008).
[8]S. Hartland, J. Colloid Interface Sci. **26**, 383 (1968).
[9]S. H. Lee, R. S. Chadwick, and L. G. Leal, J. Fluid Mech. **93**, 705 (1979).
[10]M. Manga and H. A. Stone, J. Fluid Mech. **287**, 279 (1995).
[11]J. W. J. de Folter, V. W. A. de Villeneuve, D. G. A. L. Aarts, and H. N. W. Lekkerkerker, New J. Phys. **12**, 023013 (2010).
[12]K. J. Ruschak, Annu. Rev. Fluid Mech. **17**, 65 (1985).
[13]D. Quere, Annu. Rev. Fluid Mech. **31**, 347 (1999).
[14]S. S. H. Tsai, I. M. Griffiths, and H. A. Stone, Lab Chip **11**, 2577 (2011).
[15]J. R. Anderson, D. T. Chiu, R. J. Jackman, O. Cherniavskaya, J. C. McDonald, H. K. Wu, S. H. Whitesides, and G. M. Whitesides, Anal. Chem. **72**, 3158 (2000).
[16]J. B. Knight, A. Vishwanath, J. P. Brody, and R. H. Austin, Phys. Rev. Lett. **80**, 3863 (1998).
[17]H. C. Shum, A. Sauret, A. Fernandez-Nieves, H. A. Stone, and D. A. Weitz, Phys. Fluids **22**, 082002 (2010).
[18]S. L. Anna and H. C. Mayer, Phys. Fluids **18**, 121512 (2006).
[19]See supplementary material at http://dx.doi.org/10.1063/1.3652772 for an experimental coating image with reduced speed-lag [Fig. S1]. Fig. S2 shows plots comparing the distributions of the number of beads inside one encapsulation with changing magnet distances and SDS concentration in the aqueous solution.